

Solar Model Independent Constraints on the Sterile Neutrino Interpretation of the Gallium Anomaly

M. C. Gonzalez-Garcia^{a,b,c}, Michele Maltoni^d, João Paulo Pinheiro^a

^a*Departament de Física Quàntica i Astrofísica and Institut de Ciències del Cosmos, Universitat de Barcelona, Diagonal 647, E-08028 Barcelona, Spain*

^b*Institució Catalana de Recerca i Estudis Avançats (ICREA) Pg. Lluís Companys 23 E-08010 Barcelona Spain*

^c*C.N. Yang Institute for Theoretical Physics, Stony Brook University, Stony Brook, NY 11794-3840, USA*

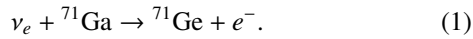
^d*Instituto de Física Teórica (IFT-CFTMAT), CSIC-UAM, Calle de Nicolás Cabrera 13–15, Campus de Cantoblanco, E-28049, Madrid, Spain*

Abstract

We perform a global analysis of most up-to-date solar neutrino data and KamLAND reactor antineutrino data in the framework of the 3+1 sterile neutrino mixing scenario (invoked to explain the results of the Gallium source experiments) with the aim of quantifying the dependence of the (in)compatibility of the required mixing with assumptions on the initial fluxes. The analysis of solar data is performed in two alternative ways: using the flux predicted by the latest standard solar models, and in a model independent approach where the solar fluxes are also determined by the fit. The dependence on the normalization of the capture rate in the solar Gallium experiments is also quantified. Similarly, in the KamLAND analysis we consider both the case where the reactor flux normalization is assumed to be known *a priori*, as well as a normalization free case which relies solely on available neutrino data. Using a parameter goodness of fit test, we find that in most cases the compatibility between Gallium and solar+KamLAND data only occur at the 3σ level or higher. We also discuss the implications of enforcing better compatibility by tweaking the mechanism for the energy production in the Sun.

1. Introduction

It is almost two decades since the so-called *Gallium Anomaly* [1, 2] became a standing puzzle in neutrino physics. In general terms, the anomaly accounts for the deficit of the event rate measured in Gallium source experiments with respect to the expectation. It was originally observed in the calibration of the gallium solar-neutrino detectors GALLEX [3, 4] and SAGE [5, 6] with radioactive ^{51}Cr and ^{37}Ar sources:



Using the detection cross section as predicted by Bahcall [7], the average ratio of observed vs predicted rates was found to be $R_{\text{GALLEX+SAGE}} = 0.88 \pm 0.05$ [6], which represented a 2.4σ statistically significant deficit. Most interestingly the Gallium Anomaly has been recently rechecked by the BEST experiment [8, 9], which placed the ^{51}Cr radioactive source at the center of a concentric two-zone gallium target (thus effectively probing two distinctive neutrino path lengths, of about 0.5 m and 1.1 m). In both zones they observe consistent deficits of $R_{\text{in}} = 0.79 \pm 0.05$ and $R_{\text{out}} = 0.77 \pm 0.05$ [8, 9], so the current combined level of the deficit is $R_{\text{GALLEX+SAGE+BEST}} = 0.80 \pm 0.05$ [8, 9] promoting the statistical significance of the anomaly beyond 4σ .

Careful scrutiny [10, 11] of the neutrino capture cross sections and its uncertainties does not provide an explanation of

the deficit, leaving open a possible effect in the neutrino propagation. The idea that ν_e may disappear during propagation from source to detector is no surprise nowadays, as the phenomenon of mass-induced neutrino flavour oscillations has been established beyond doubt (see for example the review in Ref. [12]) and the involved masses and mixing are being determined with increasing accuracy by the combined results of solar, reactor, atmospheric and long-baseline neutrino experiments (see Ref. [13] for the latest global analysis). Unfortunately, it is precisely such accuracy which puts in jeopardy the possible interpretation of the Gallium anomaly in terms of neutrino oscillations. Given the characteristic baseline $\mathcal{O}(\text{meter})$ of the GALLEX, SAGE, and BEST radioactive source experiments and their average neutrino energy $\mathcal{O}(\text{MeV})$, a $\Delta m^2 \gtrsim \mathcal{O}(\text{eV}^2)$ is required to produce visible effects, and this is more than two orders of magnitude larger than what indicated by the global analysis. Hence at least a fourth massive state must be involved in the propagation of the neutrino ensemble with mass $m_4 \sim \mathcal{O}(\text{eV})$. This in turn requires the introduction of a fourth neutrino weak eigenstate, which must be an $SU(2)$ singlet to comply with the bounds from the Z invisible width [12]. This is how the light sterile neutrino scenario makes its entrance, but in order to explain the Gallium anomaly in such way, the fourth state must significantly mix with the three standard neutrinos, $\sin^2 \theta \sim \mathcal{O}(10)\%$.

The problem is that such large mixing would impact heavily the oscillation signals included in the global analysis. This results in a strong tension between the sterile-neutrino interpretation of the Gallium anomaly and other neutrino data [14–16]. In particular solar neutrinos and reactor antineutrinos pro-

Email addresses: concha.gonzalez-garcia@stonybrook.edu

(M. C. Gonzalez-Garcia), michele.maltoni@csic.es (Michele Maltoni), joaopaulo.pinheiro@fqa.ub.edu (João Paulo Pinheiro)

vide a clean test of the possible projection of ν_e and $\bar{\nu}_e$ on a $\mathcal{O}(\text{eV})$ massive state. Given the long baselines and the energies involved, the oscillations driven by $\Delta m^2 \sim \mathcal{O}(\text{eV}^2)$ are averaged in both solar and KamLAND experiments so they directly test the mixing relevant for the interpretation of the Gallium anomaly. The analyses presented in Refs. [15, 16] lead to 2σ bounds $\sin^2 \theta \lesssim 0.025\text{--}0.045$ of the corresponding mixing angle, clearly disfavouring the sterile oscillation interpretation of the Gallium anomaly. Alternative non-conventional scenarios have also been considered (see for example Refs. [17–21]), but they are nevertheless not free from severe tension with other data [22].

It is worth noticing that the analyses of solar data in Refs. [15, 16] were performed under the assumption that the solar neutrino fluxes match the predictions of the B16 Standard Solar Models (SSM) [23]. As it is known, over the last two decades the construction of Standard Solar Models has suffered of the so called solar composition problem, associated with the choice of the input values of heavy element abundances embedded into the model. Two approaches are usually considered: either to rely on the older (and nowadays outdated) results in Ref. [24] (GS98), which imply higher metallicity and predict solar properties in good agreement with helioseismology observations, or to use the newer abundances with lower metallicity (obtained with more modern methodology and techniques) summarized in Ref. [25] (AGSS09) but which do not agree with helioseismology. This raises the question of the possible solar model dependence of the derived bounds on the sterile mixing. Addressing this issue is the subject of this work.

In this respect, recently there have been two notable developments. On the SSM building side, a new set of results (MB22 [26], based on similar methodologies and techniques as AGSS09 but with different atomic input data for the critical oxygen lines, among other differences) led to a substantial change in solar element abundances with respect to AGSS09, now more in agreement with those from GS98. Therefore, the models built following MB22 provide a good description of helioseismology results. Furthermore, as shown in Ref. [27] it is possible to perform a solar model independent analysis of the latest solar neutrino data (in combination with KamLAND) which allows for a simultaneous determination of the oscillation parameters and the normalization of the different components of the solar neutrino fluxes. The analysis in Ref. [27] was performed in the framework of 3ν oscillations, but the same methodology can be applied in the presence of mixing with a fourth sterile neutrino state, thus determining the constraints on the sterile interpretation of the Gallium anomaly in a way which is completely independent of the modelling of the Sun.

This motivates the study which we present here with the following outline. In Sec. 2 we briefly summarize the different elements entering in the analysis of solar and KamLAND data. Section 3.1 contains the results obtained in the framework of the new generation of SSMs. In Sec. 3.2 we present the results of our SSM independent analysis, subject solely to the imposition of the luminosity constraint which links together the neutrino flux and the thermal energy produced by each nuclear reaction in the Sun (and accounts for the fact that the overall amount of

generated thermal energy must match the observed solar radiated luminosity). We also comment on the implications that assuming at face value the sterile solution of the Gallium anomaly would have on the mechanism for energy production in the Sun. Finally in Sec. 4 we summarize our conclusions.

2. Framework

In the analysis of solar neutrino experiments we include the total rates from the radiochemical experiments Chlorine [28] (1 data point), Gallex/GNO [4] (2 data points), and SAGE [29] (1 data point), the spectral and day-night data from phases I-IV of Super-Kamiokande [30–33] (44, 33, 42, and 46 data points, respectively), the results of the three phases of SNO in the form of the day-night spectrum data of SNO-I [34] and SNO-II [35] and the three total rates of SNO-III [36] (34, 38, and 3 data points, respectively),¹ and the full spectra from Borexino Phase-I [39] (33 data points), Phase-II [40] (192 data points), and Phase-III [41] (120 data points), together with their latest results based on the Correlated Integrated Directionality method [42] (1 data point; see Refs. [27, 43] for details of our analysis of Borexino II and III phases). As mentioned in the introduction, an attempt to alleviate the Gallium anomaly invokes the uncertainties of the capture cross section [10, 11, 14]. This raises the issue of whether the estimated rate of solar neutrino events in Gallium experiments is really robust. To quantify the impact of such possibility, we performed two variants of our solar neutrino data analysis. In the first one we include the results of the solar Gallium experiments at their nominal values as provided by the collaboration. In the second one we introduce an additional parameter, f_{Ga} , which accounts for an overall scaling of the predicted Gallium event rates. This parameter is varied freely in the fits and mimics an energy independent modification of the capture cross section (or equivalently of the detection efficiency).

Concerning KamLAND, we include in the analysis the separate DS1, DS2, DS3 spectral data [44] (69 data points). Since KamLAND has no near detector, the theoretical uncertainties in the calculations of the reactor neutrino spectra should be dealt with some care. In the framework of 3ν oscillations as included in the latest NuFIT analysis [13], one can take advantage of the precise reactor-model independent flux determination provided by the Daya-Bay experiment [45], from which oscillation effects (calculated under the 3ν hypothesis) have been subtracted. Hence in this scenario using the Daya-Bay reactor fluxes is formally equivalent to assume that the reactor spectra and their uncertainties are known *a priori* from theoretical arguments. Conversely in the context of $3+1$ sterile oscillations the connection

¹This corresponds to the analysis labelled SNO-DATA in Ref. [37], and is at difference with Ref. [27] which used instead an alternative set (labelled SNO-POLY in Ref. [37]) based on an effective *MSW-like* polynomial parametrization for the day and night survival probabilities of the combined SNO phases I-III, as detailed in Ref. [38]. The SNO-POLY approach can be efficiently applied to 3ν oscillations but it relies on the unitarity relation $P_{ee} + P_{e\mu} + P_{e\tau} = 1$ which does not hold in the presence of extra sterile states. This leads to small quantitative differences between the results in Ref. [27] and those of this work in the limit of very small sterile neutrino mixing.

between “reactor spectra” and “Daya-Bay measurement” is no longer straightforward, and one must make some assumption about the prior knowledge of the reactor fluxes. Here we will consider two limiting cases. On the one hand, the reactor fluxes measured by Daya-Bay can be regarded as external “model” inputs and be used at face value to calculate the predictions of the KamLAND observables in the 3+1 scenario, just as one would do for 3 ν oscillations. We will label this analysis as «reactor flux constrained», or «KamLAND-RFC» in short. On the other hand, one can use the Daya-Bay reactor spectra as purely experimental inputs, taking into account that at the moment of their detection the suppression induced by the $\Delta m^2 \sim O(\text{eV}^2)$ oscillations has already taken place (so that the neutrino flux generated by the reactor cores must be proportionally larger). This is a more conservative scenario in which nothing is assumed about the theoretical prediction of the reactor flux normalization, but the implications of the Daya-Bay measurement are still taken into account. We label this analysis as «reactor flux free», or «KamLAND-RFF» in short.

In what respects the relevant survival probabilities, we focus here on a 3+1 scenario where $\{\nu_1, \nu_2, \nu_3\}$ (with mass-squared splittings Δm_{21}^2 and Δm_{31}^2 as determined by the standard 3 ν oscillation analysis) are dominantly admixtures of the left-handed states $\{\nu_e, \nu_\mu, \nu_\tau\}$, and a fourth massive state ν_4 (with a mass-squared splitting $\Delta m_{41}^2 \simeq \Delta m_{42}^2 \simeq \Delta m_{43}^2 \sim O(\text{eV}^2)$) is mostly sterile (*i.e.*, not coupled to the weak currents) but has some non-vanishing projection over the left-handed states (see appendix C of Ref. [46] for details). We obtain the oscillation probabilities for solar neutrinos by numerically solving the evolution equation for the neutrino ensemble from the neutrino production point to the detector including matter effects both in the Sun and in the Earth, with no other approximation than the assumption that the evolution in the Sun is adiabatic. We parametrize the mixing matrix as in Ref. [46, 47]:

$$U = V_{34}V_{24}V_{14}V_{23}V_{13}V_{12}, \quad (2)$$

where V_{ij} is a rotation in the ij plane by an angle θ_{ij} , which in general can also contain a complex phase (see appendix A of [46] for a discussion). Following Ref. [15] we make use of the fact that that bounds from ν_μ disappearance in atmospheric and long-baseline neutral-current measurements render the solar neutrino data effectively insensitive to θ_{34} and θ_{24} , hence in what follows we set $\theta_{34} = \theta_{24} = 0$ and obtain:

$$U = \begin{pmatrix} c_{14}c_{13}c_{12} & c_{14}c_{13}s_{12} & c_{14}s_{13} & s_{14} \\ \cdot & \cdot & \cdot & 0 \\ \cdot & \cdot & \cdot & 0 \\ -s_{14}c_{13}c_{12} & -s_{14}c_{13}s_{12} & -s_{14}s_{13} & c_{14} \end{pmatrix}. \quad (3)$$

Under these approximations and taking into account that for the distance and energies of solar and KamLAND neutrinos the oscillations driven by Δm_{31}^2 and Δm_{4i}^2 are averaged out, the relevant probabilities depend only on the three angles θ_{12} , θ_{13} , θ_{14} as well as Δm_{21}^2 . Furthermore in [46] it has been shown that the determination of θ_{13} is basically unaffected by the presence of a sterile neutrino, so we can fix it to the best fit value $s_{13}^2 = 0.02224$ obtained in the 3 ν scenario and safely neglect

its current uncertainty. Altogether the relevant probabilities depend on three parameters: Δm_{21}^2 , $\sin^2 \theta_{12}$, and $\sin^2 \theta_{14}$.

Finally, in the analysis of the Gallium source experiments one can set $\Delta m_{21}^2 = \Delta m_{31}^2 = 0$, so that the corresponding ν_e survival probability reduces to the well-known 2 ν vacuum oscillation formula and involves only two parameters, namely the large mass-squared splitting $\Delta m_{41}^2 = \Delta m_{42}^2 = \Delta m_{43}^2$ and the mixing angle θ_{14} :

$$P_{ee}^{\text{Ga-source}} = 1 - \sin^2(2\theta_{14}) \sin^2\left(\frac{\Delta m_{41}^2 L}{4E}\right). \quad (4)$$

Hence the only common parameter between the Gallium-source experiments and the solar and KamLAND experiments is θ_{14} . In what follows we will perform several compatibility tests of the oscillation parameters allowed by solar data (both alone and in combination with KamLAND) and those implied by the analysis of the Gallium source experiments. To this aim we will make use of a $\Delta\chi_{\text{Ga-source}}^2(\theta_{14})$ function inferred from the combined fit of the Gallium source experiments presented in Ref. [9].

3. Results

3.1. Updated bounds with SSM fluxes

In the first round of analyses we present the results of our fits to solar data in the framework of four different versions of the B23 standard solar models. Concretely, we consider the SSMs computed with the abundances compiled in table 5 of [26] based on the photospheric solar mixtures (MB-phot; the results obtained with meteoritic solar mixtures are totally equivalent), as well as models with the solar composition taken from Ref. [48] (AAG21), from the meteoritic scale of Ref. [25] (AGSS09-met), and from Ref. [24] (GS98).

The results of the SSM constrained analysis are presented in Fig. 1 where we plot $\Delta\chi^2(\theta_{14})$ for different choices of the solar fluxes and of the KamLAND analysis. For sake of comparison we also show $\Delta\chi_{\text{Ga-source}}^2(\theta_{14})$ as inferred from the combined fit of the Gallium source experiments presented in Ref. [9]. As can be seen all variants of the solar (+KamLAND) data analysis favour $\theta_{14} = 0$, so that the fit always results into an upper bound on the allowed range of $\sin^2 \theta_{14}$ which is in clear tension with the values required to explain the Gallium anomaly. Comparing the upper and lower panels we also see that relaxing the constraint on the normalization parameter f_{Ga} does not lead to any significant difference in the outcome. Furthermore, from the bottom-right panel we see that the fit always favour f_{Ga} close to one with 1σ uncertainty of about 7%. In comparison, the prediction of the neutrino capture cross section in Gallium in the different models can vary up to about 15% [7, 10, 11, 49–52]. This means that the global analyses of solar experiments do not support a significant modification of the neutrino capture cross section in Gallium, or any other effect inducing an energy independent reduction of the detection efficiency in the solar experiments.

The quantitative question to address is the level of (in)compatibility of these results from the solar (+KamLAND)

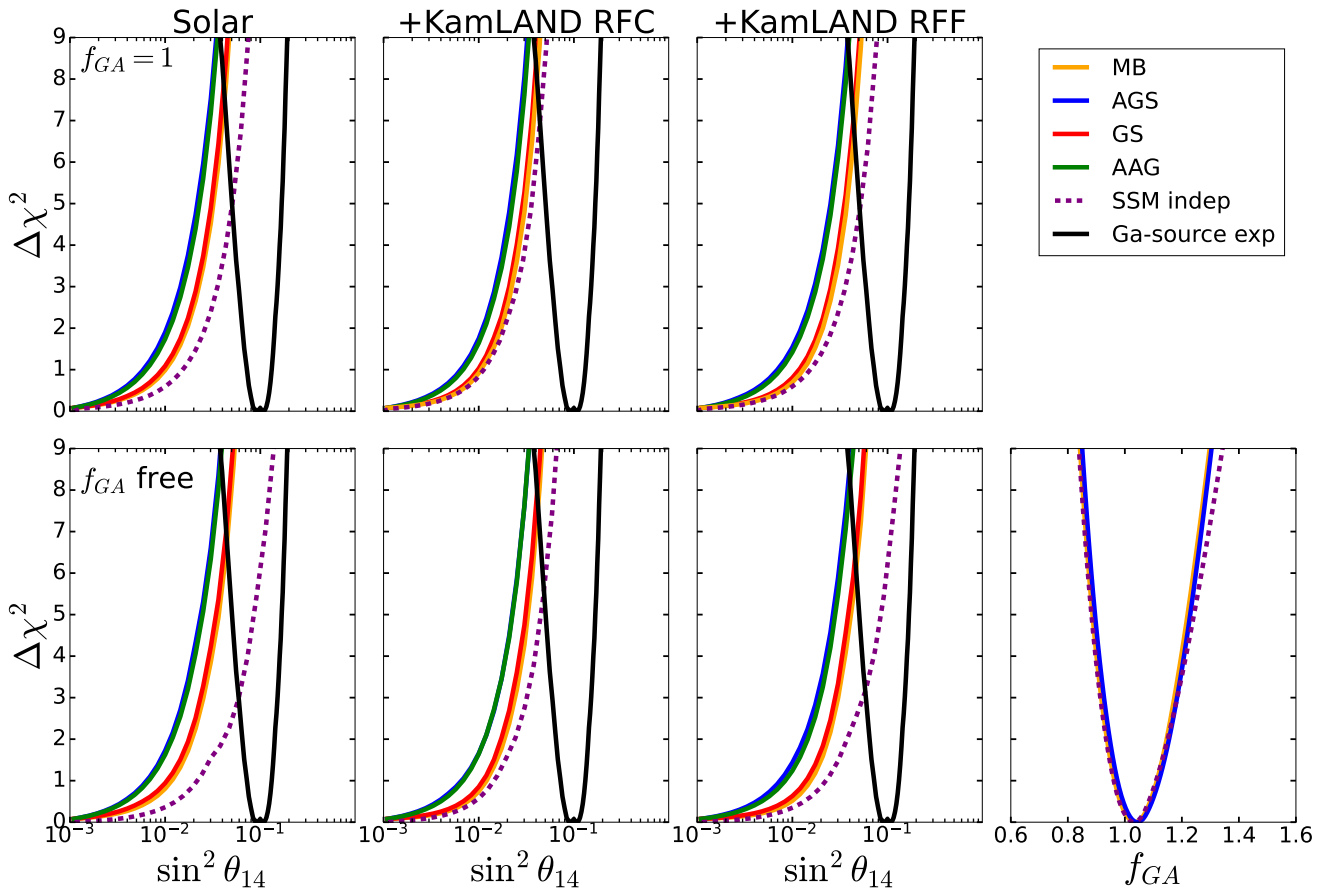


Figure 1: One-dimensional projection of the global $\Delta\chi^2$ on the mixing angle θ_{14} after marginalization over the undisplayed parameters, for different assumptions on the solar neutrino fluxes as labelled in the legend. The first (second) [third] column corresponds to the analysis including solar-only (solar+KamLAND-RFC) [solar+KamLAND-RFF] data. The upper (lower) panels show the results with $f_{\text{Ga}} = 1$ (free f_{Ga}). In all panels the black parabola is $\Delta\chi^2_{\text{Ga-source}}(\theta_{14})$ as inferred from the combined analysis of the Gallium source experiments presented in Ref. [9]. In the rightmost lower panel we show the dependence of $\Delta\chi^2$ on the normalization parameter f_{Ga} .

analysis with those from the Gallium source experiments in the context of the 3+1 scenario. Consistency among different data sets can be quantified with the parameter goodness-of-fit (PG) test [53]. For a number N of uncorrelated data sets i , each one depending on n_i model parameters and collectively depending on n_{glob} parameters, it can be shown that the test statistic

$$\chi^2_{\text{PG}} \equiv \chi^2_{\text{min, glob}} - \sum_i \chi^2_{\text{min, } i} = \min \left[\sum_i \chi_i^2 \right] - \sum_i \min \chi_i^2 \quad (5)$$

follows a χ^2 distribution with $n_{\text{PG}} \equiv \sum_i n_i - n_{\text{glob}}$ degrees of freedom [53]. In this section we have $N = 2$, and the relevant number of parameters are $n_{\text{solar(+KamLAND)}} = 3$ (or 4 for analysis with f_{Ga} free), $n_{\text{Ga-source}} = 2$ and $n_{\text{global}} = 4$ (or 5 for analysis with f_{Ga} free). So for all tests $n_{\text{PG}} = 1$, reflecting the fact that the only parameter in common between the solar (+KamLAND) and the Gallium-source data sets is θ_{14} . We list in table 1 the results of applying the PG test to the different variants of the analysis. As can be seen, the solar neutrino fits performed in the framework of the SSM's with higher (lower) metallicity are incompatible with the Gallium source experiments at the 3.6σ (4.2σ) level even when allowing for a free f_{Ga} . Combination with KamLAND results into a slight improvement or weaken-

ing of the incompatibility depending on the assumption on the reactor fluxes.

To further illustrate the interplay between solar and KamLAND data we show in Fig. 2 the two-dimensional projection of the global $\Delta\chi^2$ for the separate analysis of solar-only and KamLAND-only results under different assumptions for the corresponding input fluxes. From the upper left panel, as expected, we see that the determination of Δm_{21}^2 in KamLAND is robust irrespective of the presence of sterile neutrinos or the assumptions on the reactor flux normalization, since both occurrences only affect the overall scale of the signal whereas Δm_{21}^2 is determined by the distortions of the energy spectral shape. As it is well known from the results of the 3ν analysis, the Δm_{21}^2 values favoured by KamLAND lie in the upper 2σ allowed range of the solar neutrino fit. From the upper right panel we see that the dependence of $\Delta\chi^2_{\text{solar}}$ on θ_{14} within the Δm_{21}^2 interval favoured by KamLAND is flatter than at the lower Δm_{21}^2 values preferred by the solar-only analysis, which means that the solar-only bound on θ_{14} becomes weaker when Δm_{21}^2 is constrained to the KamLAND range. In addition, the lower panel shows that in the «KamLAND-RFF» analysis (for which no information on the absolute reactor flux normalization is included) there is

		$f_{\text{Ga}} = 1$			$f_{\text{Ga}} \text{ free}$		
	SSM	χ_{PG}^2/n	$p\text{-value} (\times 10^{-3})$	$\#\sigma$	χ_{PG}^2/n	$p\text{-value} (\times 10^{-3})$	$\#\sigma$
Solar	MB-phot/GS98	14.9	0.11	3.9	13.1	0.3	3.6
	AAG21/AGSS09	18.7	0.2	4.3	17.3	0.03	4.2
	SSM indep	9.1	2.6	3.0	4.9	27	2.2
Solar + KL-RFC	MB-phot/GS98	15.9	0.07	4.0	15.1	0.1	3.9
	AAG21/AGSS09	19.4	0.1	4.4	18.7	0.01	4.3
	SSM indep	13.5	0.23	3.7	10.5	1.2	3.2
Solar + KL-RFF	MB-phot/GS98	13.2	0.28	3.6	11.7	0.64	3.4
	AAG21/AGSS09	17.3	0.03	4.2	16.0	0.06	4.0
	SSM indep	8.7	3.1	2.9	4.8	29	2.2

Table 1: Results of the PG test for the different solar flux model assumptions and the different analysis variants.

a degeneracy between θ_{12} and θ_{14} . Such degeneracy is expected as the KamLAND survival probability in vacuum reads

$$P_{ee}^{\text{KamLAND}} \simeq \cos^4 \theta_{14} (\cos^4 \theta_{13} + \sin^4 \theta_{13}) + \sin^4 \theta_{14} - \cos^4 \theta_{14} \cos^4 \theta_{13} \sin^2(2\theta_{12}) \sin^2(\Delta m_{21}^2 L/E) \quad (6)$$

so the spectral shape of the signal only provides information on the ratio of the energy-dependent and energy-independent pieces

$$\frac{\cos^4 \theta_{14} \cos^4 \theta_{13} \sin^2(2\theta_{12})}{\cos^4 \theta_{14} (\cos^4 \theta_{13} + \sin^4 \theta_{13}) + \sin^4 \theta_{14}} \quad (7)$$

whose isocontours precisely trace the magenta lines in the $(\sin^2 \theta_{12}, \sin^2 \theta_{14})$ plane observed in the lower panel. As a consequence of all this, the combination of solar+KamLAND-RFF data leads to a slight weakening of the bounds on θ_{14} compared to the solar-only analysis, as can be seen comparing the left and right panels in Fig. 1 as well as the corresponding values of the PG test in Table 1. On the contrary the analysis of KamLAND with constrained reactor fluxes can independently bound both the numerator and denominator in Eq. (7) and therefore provides an additional constraint on θ_{14} , as illustrated by the filled green regions in the lower panel of Fig. 2. In the end when combining solar and KamLAND-RFC this second effect overcompensates the weakening of the solar bound associated with the larger Δm_{21}^2 value, so that the solar+KamLAND-RFC analysis results in a stronger θ_{14} bound than the solar-only fit.

3.2. Bounds from solar model independent analysis

As mentioned in the introduction, the combined analysis of present solar neutrino experiments and KamLAND reactor data allows for the simultaneous determination of the relevant oscillation parameters together with the normalizations Φ_i of the eight solar neutrino fluxes — five produced in the reactions of the pp-chain, $i \in \{\text{pp}, {}^7\text{Be}, \text{pep}, {}^8\text{B}, \text{hep}\}$, and three originating from the CNO-cycle, $i \in \{{}^{13}\text{N}, {}^{15}\text{O}, {}^{17}\text{F}\}$. In Ref. [27] we presented such determination in the framework of 3ν oscillations, to which we refer for the technical details. In brief, in this kind of analysis the flux normalizations are allowed to vary freely subject only to a minimal set of physical constraints and working assumptions, the most relevant of which are:

- the fluxes must be positive: $\Phi_i \geq 0$;
- the number of nuclear reactions terminating the pp-chain should not exceed the number of nuclear reactions which initiate it [54, 55]: $\Phi_{7\text{Be}} + \Phi_{8\text{B}} \leq \Phi_{\text{pp}} + \Phi_{\text{pep}}$;
- the ratio of the pep neutrino flux to the pp neutrino flux is fixed to high accuracy because they have the same nuclear matrix element, hence it is constrained to lie within a narrow range of those of the SSMs: $\Phi_{\text{pep}}/\Phi_{\text{pp}} = (1.004 \pm 0.018) \Phi_{\text{pep}}^{\text{GS98}}/\Phi_{\text{pp}}^{\text{GS98}}$;
- in what respects the CNO fluxes, we have verified that for the assessment of the (in)compatibility with the Gallium source experiments the most relevant fluxes are those of the pp-chain, and the results are very insensitive to the assumptions on the CNO fluxes. Thus, for simplicity, we have assumed a common rescaling of the three CNO fluxes with respect to those predicted by the SSM's.

In addition, the so-called ‘‘luminosity constraint’’ (*i.e.*, the requirement that the overall amount of thermal energy generated together with each neutrino flux matches the observed solar luminosity [56]) implies that

$$\frac{L_{\odot}}{4\pi (\text{A.U.})^2} = \sum_{i=1}^8 \alpha_i \Phi_i \equiv \frac{L_{\odot}(\nu\text{-inferred})}{4\pi (\text{A.U.})^2} \quad (8)$$

where α_i is the energy released by the nuclear fusion reactions associated with the i^{th} neutrino flux; its numerical value ranges from 13.099 MeV for $i = \text{pp}$ down to 3.755 MeV for $i = \text{hep}$, and is independent of the details of the solar model to an accuracy of 10^{-4} or better [55, 57]. Φ_{pp} is also the largest flux and by itself it contributes about $\sim 92\%$ of $L_{\odot}(\nu\text{-inferred})$. In Eq. (8) L_{\odot} denotes the Sun luminosity as directly extracted from the available satellite data: $L_{\odot}/[4\pi (\text{A.U.})^2] = 8.4984 \times 10^{11} \text{ MeV cm}^{-2} \text{ s}^{-1}$ [12], with an uncertainty of 0.34% due to systematics. Technically, the luminosity constraint is imposed by adding a prior to χ_{solar}^2 :

$$\chi_{\text{LC}}^2 = \left(\frac{L_{\odot}(\nu\text{-inferred})/L_{\odot} - 1}{0.0034} \right)^2. \quad (9)$$

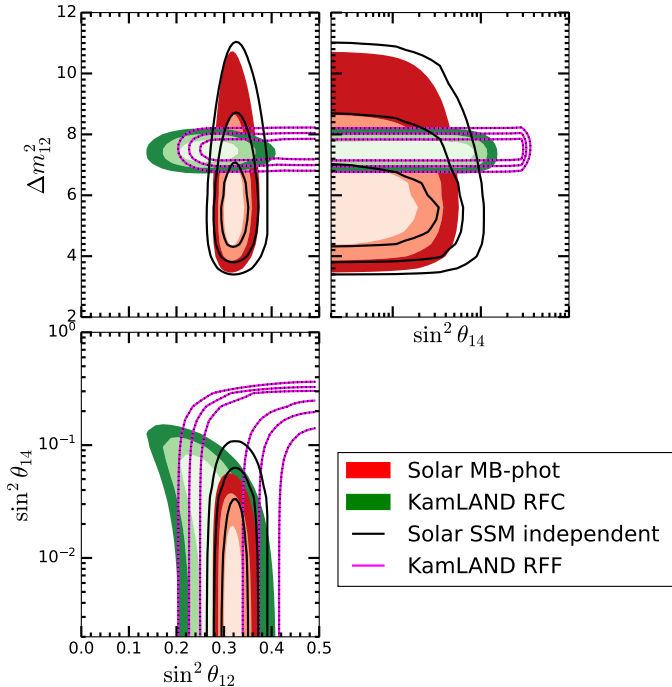


Figure 2: Two-dimensional projection of the global $\Delta\chi^2$ on the relevant oscillation parameters at 1σ , 2σ and 3σ after marginalization over the undisplayed parameters. The full red regions (void black contours) correspond to the analysis of solar data with MB-phot (free) fluxes, while the full green regions (void magenta contours) correspond to the KamLAND-RFC (KamLAND-RFF) fit.

In Fig. 2 we show as void black contours the constraints on the oscillation parameters from our SSM independent analysis of solar data, as obtained after marginalization over the various flux normalizations. Comparing these contours with the full red regions (corresponding to the analysis with solar fluxes as predicted by the MB-phot SSM) we see that the determination of the oscillation parameters is only slightly loosened in the SSM independent fit, and in particular the analysis still yields a strong bound on θ_{14} . The corresponding one-dimensional projections $\Delta\chi^2(\theta_{14})$ (both for solar-only and in combination with the two variants of the KamLAND fit) are shown as dotted lines in the various panels of Fig. 1, and the values of the PG tests are given in Table 1. From the table we read that, as long as the normalization parameter f_{Ga} is kept to its nominal value $f_{\text{Ga}} = 1$, the level of (in)compatibility between the solar (+KamLAND) data and the Gallium source experiments is at a level $\gtrsim 3\sigma$. The tension can only be relaxed to the $\sim 2.2\sigma$ level when allowing the value of f_{Ga} to float freely.

We finish by exploring the implications that assuming at face value the sterile solution of the Gallium anomaly would have on the mechanism for energy production in the Sun as inferred from neutrino data. As mentioned above, pp neutrinos yield the largest contribution both to $L_\odot(\nu\text{-inferred})$ ($\gtrsim 90\%$) and to the event rate of the Gallium solar experiments ($\gtrsim 55\%$), which poses the question of what should be the deviation from the relation in Eq. (8) required for solar observations to be compatible with the Gallium source experimental results. In order to quantitatively answer this question we have performed a SSM independent analysis similar to the one described above, but

without imposing the prior in Eq. (9). This allows us to determine the level of compatibility between solar+KamLAND data and Gallium source experiments as a function of the ν -inferred solar luminosity, by comparing the $\sin^2\theta_{14}$ range preferred by each data set. The results are shown in Fig. 3. In the left panel we plot the 1σ , 2σ , 3σ (1 dof) ranges for θ_{14} (defined with respect to the global minimum) allowed by the combined fit of solar and KamLAND data (for both variants of the KamLAND analysis) as a function of the ν -inferred solar luminosity in units of the directly observed L_\odot . For comparison we show as horizontal grey bands the corresponding required ranges to explain the Gallium anomaly. As seen in the figure, for either analysis, compatibility requires a substantial deviation of the luminosity inferred from the solar neutrino observations with respect to its value as directly determined. This is further quantified in the right panel, which shows the increase in χ^2 when combining together solar+KamLAND and Ga-source data (as a function of the aforesaid luminosity ratio) with respect to the sum of the two separate best-fits (so that by construction the minimum of each curve yields the χ^2_{PG} value defined in Eq. (5)). As seen in the figure, for the KamLAND-RFC case the level of compatibility is always higher than 2.8σ , while in the KamLAND-RFF case the compatibility only drops below the 2σ level if one allows $L_\odot(\nu\text{-inferred})$ to deviate by more than 10% from the directly determined solar luminosity. In other words, to accommodate the sterile neutrino interpretation of the Gallium anomaly within the present observation of solar and KamLAND neutrinos at better than the 2σ level, it is necessary to (a) make no assumption on the normalization of the reactor antineutrino fluxes, and (b) accept that more than 10% of the energy produced in the nuclear reactions in the Sun does *not* result into observed radiation — despite the fact that, as mentioned before, the solar radiated luminosity is directly determined with 0.34% precision.

4. Summary

In this work we have presented a variety of global analyses of solar neutrino data (both alone and in combination with the KamLAND reactor antineutrino results) in the framework of the 3+1 neutrino mixing scenario commonly invoked to explain the results from Gallium source experiments. With these fits at hand, we have performed consistency tests to assess the level of (in)compatibility between the range of the sterile neutrino mixing preferred by each data set, and we have studied the dependence of the results on the different assumptions entering in the analysis. All the fits considered here have shown compatibility (as measured by the parameter goodness-of-fit) only at the 3σ level or higher. This conclusion holds for analyses assuming solar neutrino fluxes as predicted by any of the last generation Standard Solar Models, and irrespective of the assumptions on the KamLAND reactor flux normalization and on the gallium capture rate. Relaxing the SSM constraints on the solar fluxes — while still enforcing the relation between the observed value of the solar radiated luminosity and the total amount of thermal energy generated by the various neutrino-emitting nuclear reactions — only improves the compatibility to levels below 3σ

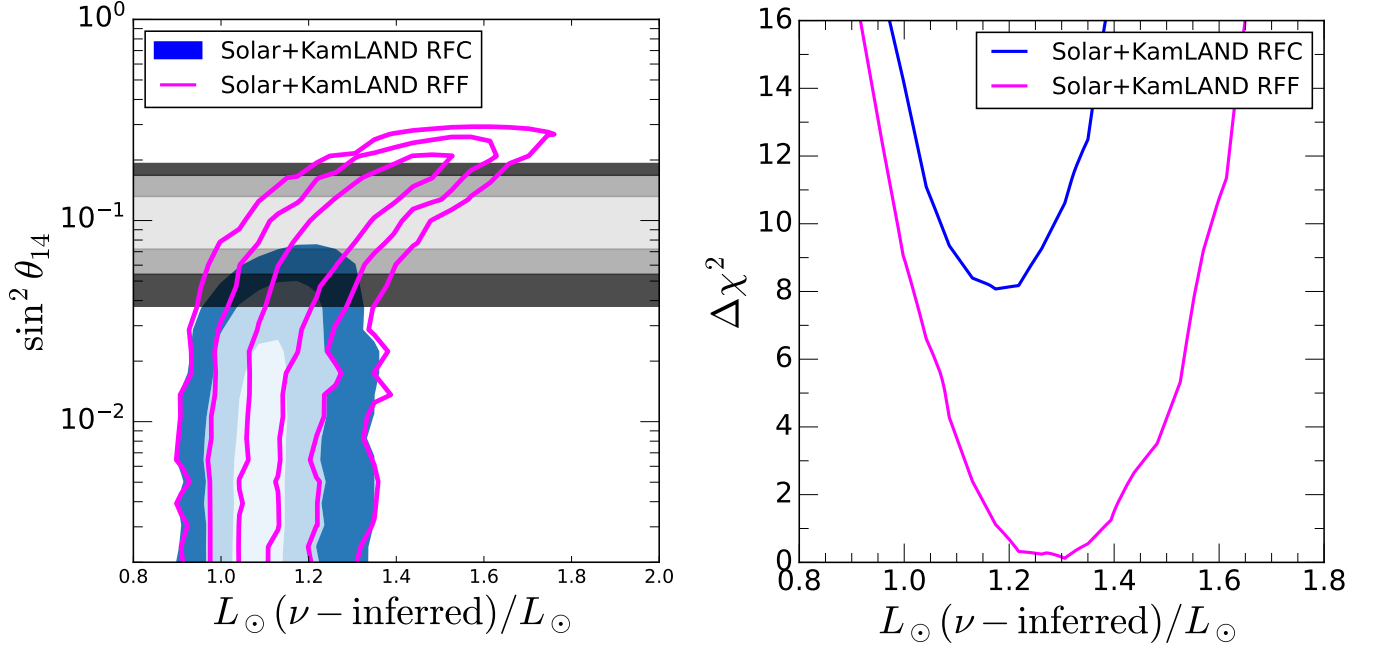


Figure 3: Left: dependence of the 1σ , 2σ , 3σ ranges of $\sin^2 \theta_{14}$ from the analysis of solar+KamLAND without imposing the constraint in Eq. (9) on the resulting neutrino-inferred solar luminosity. Fill (void) regions correspond to solar+KamLAND-RFC (solar+KamLAND-RFF) analysis. The horizontal grey regions illustrate the 1σ , 2σ , 3σ ranges required to explain the Gallium source results. Right: value of $\Delta\chi^2$ from the joint analysis of solar+KamLAND and Ga-source data, defined with respect to the sum of the two separate best-fit χ^2_{\min} , as a function of the neutrino-inferred solar luminosity.

when no prior knowledge in either the gallium capture rate or the normalization of reactor neutrino fluxes is assumed. If the luminosity constraint is also dropped, then it is formally possible to achieve a compatibility level below 2σ as long as the flux of reactor antineutrinos is left free, but such solution unavoidably requires that more than 10% of the energy produced together with neutrinos in the nuclear reactions of the Sun does not result into observable radiation.

Acknowledgements

This project is funded by USA-NSF grant PHY-1915093 and by the European Union through the Horizon 2020 research and innovation program (Marie Skłodowska-Curie grant agreement 860881-HIDDeN) and the Horizon Europe programme (Marie Skłodowska-Curie Staff Exchange grant agreement 101086085-ASYMMETRY). It also receives support from grants PID2020-113644GB-I00, PID2022-142545NB-C21, “Unit of Excellence Maria de Maeztu 2020-2023” award to the ICC-UB CEX2019-000918-M, “Unit of Excellence Maria de Maeztu 2021-2025” award to ICE CEX2020-001058-M, grant IFT “Centro de Excelencia Severo Ochoa” CEX2020-001007-S funded by MCIN/AEI/10.13039/501100011033, as well as from grants 2021-SGR-249 and 2021-SGR-1526 (Generalitat de Catalunya).

References

- [1] C. Giunti, M. Laveder, Short-Baseline Active-Sterile Neutrino Oscillations?, *Mod. Phys. Lett. A* 22 (2007) 2499–2509. [arXiv:hep-ph/0610352](#), [doi:10.1142/S0217732307025455](#).
- [2] M. Laveder, Unbound neutrino roadmaps, *Nucl. Phys. B Proc. Suppl.* 168 (2007) 344–346. [doi:10.1016/j.nuclphysbps.2007.02.037](#).
- [3] W. Hampel, et al., Final results of the Cr-51 neutrino source experiments in GALLEX, *Phys. Lett. B* 420 (1998) 114–126. [doi:10.1016/S0370-2693\(97\)01562-1](#).
- [4] F. Kaether, W. Hampel, G. Heusser, J. Kiko, T. Kirsten, Reanalysis of the GALLEX solar neutrino flux and source experiments, *Phys. Lett. B* 685 (2010) 47–54. [arXiv:1001.2731](#), [doi:10.1016/j.physletb.2010.01.030](#).
- [5] J. N. Abdurashitov, et al., Measurement of the response of the Russian-American gallium experiment to neutrinos from a Cr-51 source, *Phys. Rev. C* 59 (1999) 2246–2263. [arXiv:hep-ph/9803418](#), [doi:10.1103/PhysRevC.59.2246](#).
- [6] J. N. Abdurashitov, et al., Measurement of the response of a Ga solar neutrino experiment to neutrinos from an Ar-37 source, *Phys. Rev. C* 73 (2006) 045805. [arXiv:nuc1-ex/0512041](#), [doi:10.1103/PhysRevC.73.045805](#).
- [7] J. N. Bahcall, Gallium solar neutrino experiments: Absorption cross-sections, neutrino spectra, and predicted event rates, *Phys. Rev. C* 56 (1997) 3391–3409. [arXiv:hep-ph/9710491](#), [doi:10.1103/PhysRevC.56.3391](#).
- [8] V. V. Barinov, et al., Results from the Baksan Experiment on Sterile Transitions (BEST), *Phys. Rev. Lett.* 128 (23) (2022) 232501. [arXiv:2109.11482](#), [doi:10.1103/PhysRevLett.128.232501](#).
- [9] V. V. Barinov, et al., Search for electron-neutrino transitions to sterile states in the BEST experiment, *Phys. Rev. C* 105 (6) (2022) 065502. [arXiv:2201.07364](#), [doi:10.1103/PhysRevC.105.065502](#).
- [10] S. R. Elliott, V. N. Gavrin, W. C. Haxton, T. V. Ibragimova, E. J. Rule, Gallium neutrino absorption cross section and its uncertainty, *Phys. Rev. C* 108 (3) (2023) 035502. [arXiv:2303.13623](#), [doi:10.1103/PhysRevC.108.035502](#).
- [11] C. Giunti, Y. F. Li, C. A. Ternes, Z. Xin, Inspection of the detection cross section dependence of the Gallium Anomaly, *Phys. Lett. B* 842 (2023) 137983. [arXiv:2212.09722](#), [doi:10.1016/j.physletb.2023.137983](#).
- [12] S. Navas, et al., Review of particle physics, *Phys. Rev. D* 110 (3) (2024) 030001. [doi:10.1103/PhysRevD.110.030001](#).
- [13] I. Esteban, M. C. Gonzalez-Garcia, M. Maltoni, I. Martinez-Soler, J. a. P.

- Pinheiro, T. Schwetz, NuFit-6.0: Updated global analysis of three-flavor neutrino oscillations (10 2024). [arXiv:2410.05380](#).
- [14] J. M. Berryman, P. Coloma, P. Huber, T. Schwetz, A. Zhou, Statistical significance of the sterile-neutrino hypothesis in the context of reactor and gallium data, *JHEP* 02 (2022) 055. [arXiv:2111.12530](#), doi:10.1007/JHEP02(2022)055.
- [15] K. Goldhagen, M. Maltoni, S. E. Reichard, T. Schwetz, Testing sterile neutrino mixing with present and future solar neutrino data, *Eur. Phys. J. C* 82 (2) (2022) 116. [arXiv:2109.14898](#), doi:10.1140/epjc/s10052-022-10052-2.
- [16] C. Giunti, Y. F. Li, C. A. Ternes, O. Tyagi, Z. Xin, Gallium Anomaly: critical view from the global picture of ν_e and $\bar{\nu}_e$ disappearance, *JHEP* 10 (2022) 164. [arXiv:2209.00916](#), doi:10.1007/JHEP10(2022)164.
- [17] V. Brdar, J. Gehrlein, J. Kopp, Towards resolving the gallium anomaly, *JHEP* 05 (2023) 143. [arXiv:2303.05528](#), doi:10.1007/JHEP05(2023)143.
- [18] Y. Farzan, T. Schwetz, A decoherence explanation of the gallium neutrino anomaly, *SciPost Phys.* 15 (4) (2023) 172. [arXiv:2306.09422](#), doi:10.21468/SciPostPhys.15.4.172.
- [19] C. A. Argüelles, T. Bertólez-Martínez, J. Salvado, Impact of wave packet separation in low-energy sterile neutrino searches, *Phys. Rev. D* 107 (3) (2023) 036004. [arXiv:2201.05108](#), doi:10.1103/PhysRevD.107.036004.
- [20] J. M. Hardin, I. Martínez-Soler, A. Diaz, M. Jin, N. W. Kamp, C. A. Argüelles, J. M. Conrad, M. H. Shaevitz, New Clues about light sterile neutrinos: preference for models with damping effects in global fits, *JHEP* 09 (2023) 058. [arXiv:2211.02610](#), doi:10.1007/JHEP09(2023)058.
- [21] H. Banks, K. J. Kelly, M. McCullough, T. Zhou, Broad sterile neutrinos & the reactor/gallium tension, *JHEP* 04 (2024) 096. [arXiv:2311.06352](#), doi:10.1007/JHEP04(2024)096.
- [22] C. Giunti, C. A. Ternes, Confronting solutions of the Gallium Anomaly with reactor rate data, *Phys. Lett. B* 849 (2024) 138436. [arXiv:2312.00565](#), doi:10.1016/j.physletb.2023.138436.
- [23] N. Vinyoles, A. M. Serenelli, F. L. Villante, S. Basu, J. Bergström, M. C. Gonzalez-Garcia, M. Maltoni, C. Peña Garay, N. Song, A new Generation of Standard Solar Models, *Astrophys. J.* 835 (2) (2017) 202. [arXiv:1611.09867](#), doi:10.3847/1538-4357/835/2/202.
- [24] N. Grevesse, A. J. Sauval, Standard Solar Composition, *Space Sci. Rev.* 85 (1998) 161–174. doi:10.1023/A:1005161325181.
- [25] M. Asplund, N. Grevesse, A. J. Sauval, P. Scott, The Chemical Composition of the Sun, *ARA&A* 47 (1) (2009) 481–522. [arXiv:0909.0948](#), doi:10.1146/annurev.astro.46.060407.145222.
- [26] E. Magg, et al., Observational constraints on the origin of the elements - IV. Standard composition of the Sun, *Astron. Astrophys.* 661 (2023) A140. [arXiv:2203.02255](#), doi:10.1051/0004-6361/202142971.
- [27] M. C. Gonzalez-Garcia, M. Maltoni, J. a. P. Pinheiro, A. M. Serenelli, Status of direct determination of solar neutrino fluxes after Borexino, *JHEP* 02 (2024) 064. [arXiv:2311.16226](#), doi:10.1007/JHEP02(2024)064.
- [28] B. T. Cleveland, et al., Measurement of the solar electron neutrino flux with the Homestake chlorine detector, *Astrophys. J.* 496 (1998) 505–526. doi:10.1086/305343.
- [29] J. N. Abdurashitov, et al., Measurement of the solar neutrino capture rate with gallium metal. III: Results for the 2002–2007 data-taking period, *Phys. Rev. C* 80 (2009) 015807. [arXiv:0901.2200](#), doi:10.1103/PhysRevC.80.015807.
- [30] J. Hosaka, et al., Solar neutrino measurements in Super-Kamiokande-I, *Phys. Rev. D* 73 (2006) 112001. [arXiv:hep-ex/0508053](#), doi:10.1103/PhysRevD.73.112001.
- [31] J. Cravens, et al., Solar neutrino measurements in Super-Kamiokande-II, *Phys. Rev. D* 78 (2008) 032002. [arXiv:0803.4312](#), doi:10.1103/PhysRevD.78.032002.
- [32] K. Abe, et al., Solar neutrino results in Super-Kamiokande-III, *Phys. Rev. D* 83 (2011) 052010. [arXiv:1010.0118](#), doi:10.1103/PhysRevD.83.052010.
- [33] K. Abe, et al., Solar neutrino measurements using the full data period of Super-Kamiokande-IV, *Phys. Rev. D* 109 (9) (2024) 092001. [arXiv:2312.12907](#), doi:10.1103/PhysRevD.109.092001.
- [34] B. Aharmim, et al., Measurement of the ν_e and total B-8 solar neutrino fluxes with the Sudbury Neutrino Observatory phase I data set, *Phys. Rev. C* 75 (2007) 045502. [arXiv:nucl-ex/0610020](#), doi:10.1103/PhysRevC.75.045502.
- [35] B. Aharmim, et al., Electron energy spectra, fluxes, and day-night asymmetries of B-8 solar neutrinos from the 391-day salt phase SNO data set, *Phys. Rev. C* 72 (2005) 055502. [arXiv:nucl-ex/0502021](#), doi:10.1103/PhysRevC.72.055502.
- [36] B. Aharmim, et al., An Independent Measurement of the Total Active 8B Solar Neutrino Flux Using an Array of 3He Proportional Counters at the Sudbury Neutrino Observatory, *Phys. Rev. Lett.* 101 (2008) 111301. [arXiv:0806.0989](#), doi:10.1103/PhysRevLett.101.111301.
- [37] M. C. Gonzalez-Garcia, M. Maltoni, Determination of matter potential from global analysis of neutrino oscillation data, *JHEP* 09 (2013) 152. [arXiv:1307.3092](#), doi:10.1007/JHEP09(2013)152.
- [38] B. Aharmim, et al., Combined Analysis of all Three Phases of Solar Neutrino Data from the Sudbury Neutrino Observatory (2011). [arXiv:1109.0763](#).
- [39] G. Bellini, et al., Precision measurement of the 7Be solar neutrino interaction rate in Borexino, *Phys. Rev. Lett.* 107 (2011) 141302. [arXiv:1104.1816](#), doi:10.1103/PhysRevLett.107.141302.
- [40] M. Agostini, et al., First Simultaneous Precision Spectroscopy of pp , ${}^7\text{Be}$, and pep Solar Neutrinos with Borexino Phase-II, *Phys. Rev. D* 100 (8) (2019) 082004. [arXiv:1707.09279](#), doi:10.1103/PhysRevD.100.082004.
- [41] S. Appel, et al., Improved Measurement of Solar Neutrinos from the Carbon-Nitrogen-Oxygen Cycle by Borexino and Its Implications for the Standard Solar Model, *Phys. Rev. Lett.* 129 (25) (2022) 252701. [arXiv:2205.15975](#), doi:10.1103/PhysRevLett.129.252701.
- [42] D. Basilico, et al., Final results of Borexino on CNO solar neutrinos (7 2023). [arXiv:2307.14636](#).
- [43] P. Coloma, M. Gonzalez-Garcia, M. Maltoni, J. a. P. Pinheiro, S. Urrea, Constraining new physics with Borexino Phase-II spectral data, *JHEP* 07 (2022) 138, [Erratum: *JHEP* 11, 138 (2022)]. [arXiv:2204.03011](#), doi:10.1007/JHEP07(2022)138.
- [44] A. Gando, et al., Reactor On-Off Antineutrino Measurement with KamLAND, *Phys. Rev. D* 88 (3) (2013) 033001. [arXiv:1303.4667](#), doi:10.1103/PhysRevD.88.033001.
- [45] F. P. An, et al., Antineutrino energy spectrum unfolding based on the Daya Bay measurement and its applications, *Chin. Phys. C* 45 (7) (2021) 073001. [arXiv:2102.04614](#), doi:10.1088/1674-1137/abfc38.
- [46] J. Kopp, P. A. N. Machado, M. Maltoni, T. Schwetz, Sterile Neutrino Oscillations: The Global Picture, *JHEP* 05 (2013) 050. [arXiv:1303.3011](#), doi:10.1007/JHEP05(2013)050.
- [47] M. Dentler, A. Hernández-Cabezudo, J. Kopp, P. A. N. Machado, M. Maltoni, I. Martínez-Soler, T. Schwetz, Updated Global Analysis of Neutrino Oscillations in the Presence of eV-Scale Sterile Neutrinos, *JHEP* 08 (2018) 010. [arXiv:1803.10661](#), doi:10.1007/JHEP08(2018)010.
- [48] M. Asplund, A. M. Amarsi, N. Grevesse, The chemical make-up of the Sun: A 2020 vision, *arXiv e-prints* (2021) [arXiv:2105.01661](#) [arXiv:2105.01661](#).
- [49] W. C. Haxton, Cross-section uncertainties in the gallium neutrino source experiments, *Phys. Lett. B* 431 (1998) 110–118. [arXiv:nucl-th/9804011](#), doi:10.1016/S0370-2693(98)00581-4.
- [50] D. Frekers, et al., Precision evaluation of the ${}^{71}\text{Ga}$ solar neutrino capture rate from the (${}^3\text{He}, t$) charge-exchange reaction, *Phys. Rev. C* 91 (3) (2015) 034608, [Erratum: *Phys. Rev. C* 100, 049901 (2019)]. doi:10.1103/PhysRevC.91.034608.
- [51] J. Kostensalo, J. Suhonen, C. Giunti, P. C. Srivastava, The gallium anomaly revisited, *Phys. Lett. B* 795 (2019) 542–547. [arXiv:1906.10980](#), doi:10.1016/j.physletb.2019.06.057.
- [52] S. V. Semenov, Cross Section of Neutrino Absorption by the Gallium-71 Nucleus, *Phys. Atom. Nucl.* 83 (11) (2020) 1549–1552. doi:10.1134/S1063778820100221.
- [53] M. Maltoni, T. Schwetz, Testing the statistical compatibility of independent data sets, *Phys. Rev. D* 68 (2003) 033020. [arXiv:hep-ph/0304176](#), doi:10.1103/PhysRevD.68.033020.
- [54] J. N. Bahcall, P. I. Krastev, How well do we (and will we) know solar neutrino fluxes and oscillation parameters?, *Phys. Rev. D* 53 (1996) 4211–4225. [arXiv:hep-ph/9512378](#), doi:10.1103/PhysRevD.53.4211.
- [55] J. N. Bahcall, The Luminosity constraint on solar neutrino fluxes, *Phys. Rev. C* 65 (2002) 025801. [arXiv:hep-ph/0108148](#), doi:10.1103/PhysRevC.65.025801.

- [56] M. Spiro, D. Vignaud, Solar Model Independent Neutrino Oscillation Signals in the Forthcoming Solar Neutrino Experiments?, *Phys. Lett. B* 242 (1990) 279–284, [,609(1990)]. doi:10.1016/0370-2693(90)91471-M.
- [57] D. Vescovi, C. Mascaretti, F. Vissani, L. Piersanti, O. Straniero, The luminosity constraint in the era of precision solar physics, *Journal of Physics G Nuclear Physics* 48 (1) (2021) 015201. arXiv:2009.05676, doi:10.1088/1361-6471/abb784.